Buffer Insensitive Optoelectronic Quality of InP-on-Si with Templated Liquid Phase Growth

Debarghya Sarkar, Wei Wang, Qingfeng Lin, Jun Tao

Ming Hsieh Department of Electrical Engineering, University of Southern California, Los Angeles, California 90089, United States

Matthew Mecklenburg

Center for Electron Microscopy and Microanalysis, University of Southern California, Los Angeles, California 90089, United States

Jayakanth Ravichandran

Mork Family Department of Chemical Engineering and Materials Science, University of Southern California, Los Angeles, California 90089, United States

Rehan Kapadia[a)]

Ming Hsieh Department of Electrical Engineering, University of Southern California, Los Angeles, California 90089, United States

[a)] Electronic mail: rkapadia@usc.edu

16 September 2024 05:21:45

As Moore's Law comes to an end, the search for additional integrated circuit functionality has shifted from scaling lateral dimensions down to combining multiple materials onto a single substrate. However, the quality of crystalline semiconductors is highly sensitive to the substrate upon which it is grown, preventing multiple materials from being directly

grown on single substrates. To circumvent this challenge, many complex growth strategies have been developed, such as strain relaxation buffer-layers, nanostructure growth, and template selective epitaxy. However, even with these advanced growth technique, the growth of manufacturable crystalline materials is still limited to crystalline surfaces. Here, we show that using templated liquid phase (TLP) growth, single crystalline indium phosphide on Si can be grown using a variety of buffers, both crystalline and amorphous. However, by performing detailed optoelectronic characterization, we find that the quality of the grown material not only closely matches commercial single crystalline InP wafers but is also highly *insensitive* to the buffer layer used. This unique feature of TLP growth could enable the next generation of crystalline material integration.

I. INTRODUCTION

Conventionally, compound semiconductor films are grown using vapor-phase growth techniques[1,2] by coalescence of multiple nucleation sites on the substrate. Films grown on amorphous substrates with no long-range order would therefore be small-grain polycrystalline with inferior electronic and optoelectronic quality. High quality single crystalline films from vapor-phase growths necessitates the use of lattice matched substrates, thereby stifling the massive application potential owing to economic and substrate specificity constraints. Recently, we have demonstrated the growth of single-crystalline templated thin films of compound semiconductors on an array of arbitrary substrates[3-7] using vapor-liquid-solid growth from constrained liquid templates. As described in our previous works, this growth technology advances the repertoire of thin film growth in multiple ways. First, it allows one to grow large-scale (several tens of micron) single-crystal templates of compound semiconductors on arbitrary substrates, of

16 September 2024 05:21:45

optoelectronic quality comparable to that of a standard commercial wafer. Second, the final geometry of the crystal is pre-determined by the shape of the templated metal unlike that in standard vapor phase growth methods, where it is affected by the growth rates of the respective crystal facets. These have far-reaching implications in the fabrication of high performance devices and their integration on different substrates for varying applications such as optical metasurfaces[8], photonic integrated circuits[9], high carrier mobility electronics[10]. Essentially, this renders a palette of material and geometry options to the device engineer to design a system giving priority to the device performance over material growth constraints.

In this work we explore the growth condition optimization of optoelectronic properties of TLP InP grown on crystalline and amorphous insulators on silicon, with a commercial single crystalline wafer as the reference. Specifically, we performed detailed luminescence studies, with the peak position, full width at half maximum (FWHM), and Urbach parameter as the metrics. At the optimal growth condition, we observe nearly identical optoelectronic properties between our InP on Si and the single crystalline wafer. Importantly, we carry out a statistical analysis on the uniformity and reproducibility of the material grown here and, show that the InP grown with this technique has extremely narrow dispersion in optoelectronic properties. Given that this material was grown in a simple quartz tube furnace with no regard to controlling gas flow, this is important evidence pointing to the potentially improved scalability of this approach as compared to standard vapor-solid approaches that require complex gas flow control to achieve material uniformity across wafers.

II. EXPERIMENTAL

16 September 2024 05:21:45

A. Templated Liquid Phase Growth

We followed the fabrication procedure as shown schematically in Figure 1.

Thermal evaporation of indium (99.99995%) was done on the lithographically patterned

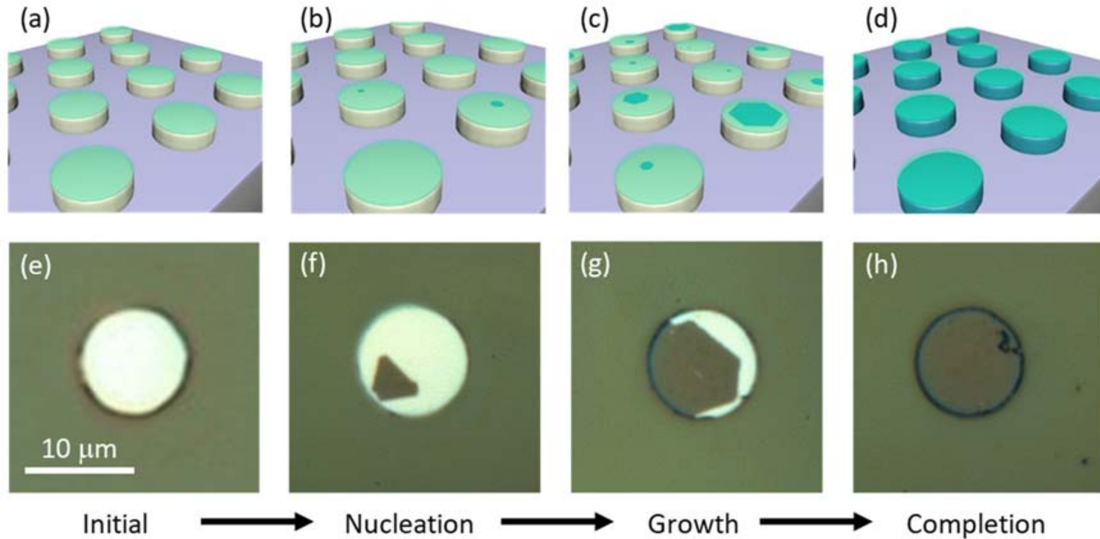

Figure 1. (Color online) (a-d) Schematic of TLP crystal growth process. (e-h) Optical microscope image of a representative template showing different stages of TLP crystal growth.

samples attached to a stage maintained at cryogenic temperature by liquid nitrogen cooling. This was followed by electron-beam evaporation of a capping layer of SiO_2. Templates of In/SiO_2 stacks were obtained by standard lift-off process. This is schematically represented in Figure 1 (a). Figure 1 (e) is a top view optical microscope image of a single In/SiO_2 template. Each template is a circular pattern of 10 μm diameter with a center to center spacing of 30 μm between templates. The indium thickness is 500 nm In and the SiO_2 thickness is 100nm. Once the initial patterns were obtained, the entire substrate was heated up in vacuum in a single-zone hot-wall tube furnace (Lindberg Blue) above the melting point of indium to the chosen growth temperature, between 450

16 September 2024 05:21:45

^{0}C and 750 ^{0}C. At the growth temperatures, a gas phase phosphine/hydrogen mixture was introduced into the growth chamber, resulting in phosphorus diffusion into the liquid indium. Supersaturation of phosphorus in liquid indium leads to a chemical phase transformation and precipitation of indium phosphide to drive the remaining melt towards equilibrium. Based on some of the previous reports of the TLP growth[3-5], the gas flux was controlled to ensure single nucleation sites in individual mesas, schematically portrayed in Figure 1 (b), and a typical example of which is shown in Figure 1 (f). 5 sccm PH_3 (99.9995%, Matheson) was used as the P precursor, diluted with 99.999% H_2 to achieve the desired PH_3 partial pressure (5 to 50 torr), with the total pressure being 100 torr. Subsequent consumption of indium and precipitation of InP therefore leads to the growth of a single crystal from each mesa. Figure 1 (c) is a schematic snapshot of the partially grown InP mesas, specifically depicting single crystal growth in each mesa, and Figure 1 (g) is a representative top view optical microscope image of a single template. With sufficient growth time, the entire indium mesa is consumed, and turned to InP, as shown in Figures 1 (d) and (h). As also mentioned earlier, the geometry of the resulting material is determined by the geometry of the original growth template, and is not controlled by the relative growth rates of the individual crystal facets. Also, the primary out of plane crystal orientation of the InP growth was found to be (111), regardless of the substrate[5]. After growth, the SiO_2 capping layer is selectively etched in hydrofluoric acid (HF) solution leaving behind the grown InP mesa.

B. Structural and optoelectronic characterization

Figures 2 (a) and (b) are cross-sectional TEM micrographs of InP mesa grown on top of Gd_2O_3/Si and TiO_2/SiO_2/Si substrate, respectively, demonstrating growth of

16 September 2024 05:21:45

uniform InP on both crystalline and amorphous dielectric surfaces. A plan view false color SEM image of a matrix of fully grown InP mesas on a dielectric substrate after HF etching of the top SiO_2 capping layer, is shown in Figure 2 (c). Extensive micro-photoluminescence measurements and analysis were carried out to characterize the optoelectronic quality of the grown materials. Steady state photoluminescence (PL) measurements have been carried out in a Renishaw inVia confocal Raman Microscope setup using a constant power 532nm laser source as the excitation and Si CCD detector. A representative photoluminescence curve of the InP grown by the TLP method, is shown in Figure 2 (d), with optoelectronic quality in terms of peak position, FWHM, and Urbach parameter comparable to that of a commercial single crystal n-type (5-6e16 cm^{-3}) InP wafer. The inset shows the comparison of absolute intensities between the InP grown by the TLP method and that of the single crystal commercial wafer under same excitation conditions.

16 September 2024 05:21:45

1. Photoluminescence analysis

Photoluminescence spectra from materials grown at different temperatures were analyzed to extract peak position, full width at half maximum (FWHM), and Urbach parameter as metrics for optoelectronic quality comparison. Nominally the peak luminescence occurs at the bandgap energy of the semiconductor. But the peak position may blue shift (called Burstein-Moss shift) because of doping of the semiconductor leading to an effective shift in the energy level with available states[11,12]. A red shift in the peak position may be caused by presence of charge traps in the bandgap with long lifetime. Density of states in the bandgap arise from defects, thermal vibrations and charged impurities[13,14]. The semilog inverse slope of the absorption in the bandgap is the

Urbach parameter, which represents the exponential decay rate of the density of states in the bandgap. Thus, a smaller value of Urbach parameter implies a material with lower defect density and ionized impurity concentrations. Details of Urbach parameter extraction procedure are described below.

The relation between the optical emission rate per unit energy $R(hv)$ and the absorption coefficient $\alpha(hv)$, is given by the van Roosbroeck-Schockley equation[15]

$$R(hv) = \alpha(hv) \frac{8\pi v^2 n^2}{hc^2 (e^{hv/kT} - 1)}$$

where $R(hv)$ is the emission intensity, v is frequency, n is the refractive index of InP, h is Planck's constant, c is the speed of light in vacuum, k is Boltzmann's constant, T is absolute temperature.

At the bandgap energies where the absorption coefficient is small, the (external) photoluminescence spectrum $P(hv)$ may be approximated to have a similar shape to that of the emission spectrum, independent of the thickness of the sample. Thus, the van Roosbroeck-Shockley equation may be represented as[16]

$$\alpha(hv) \propto P(hv) \frac{(e^{hv/kT} - 1)}{n^2 (hv)^2}$$

The absorption coefficient in the bandgap varies exponentially with energy[17], so that we can fit it with an equation of the form

$$\alpha(hv) = \alpha_0 e^{(E - E_{ref})/E_0}$$

where α_0 and E_0 are fitting parameters, and E_{ref} is a reference energy, here taken to be the InP bandgap energy, 1.34 eV. The term E_0 is referred to as Urbach parameter, and represents the sharpness of the exponentially decreasing absorption in the bandgap.

16 September 2024 05:21:45

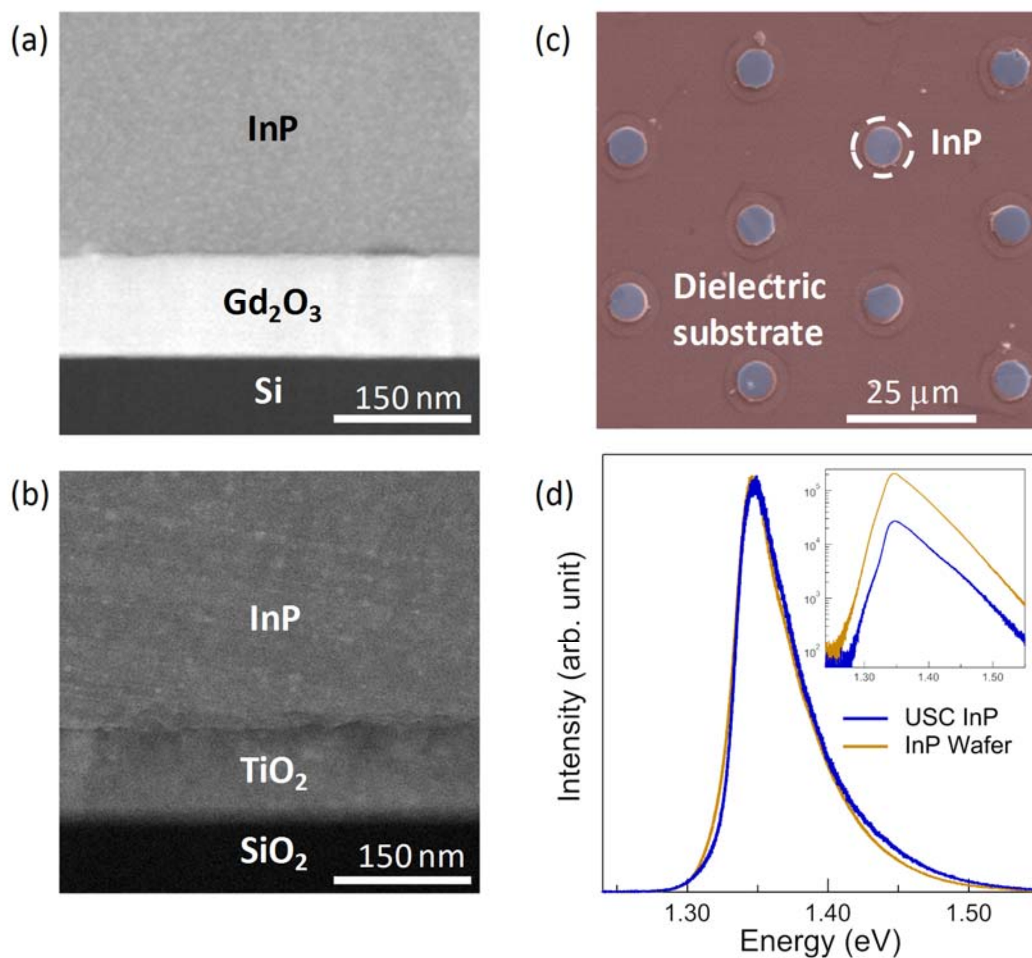

Figure 2. (Color online) (a) Cross-section TEM of InP on crystalline Gd_2O_3 film on Si. (b) Cross-section TEM of InP on amorphous TiO2 film on Si/ SiO_2. (c) Top-view SEM of InP templates on dielectric substrate. (d) Representative photoluminescence spectrum of USC InP compared with InP wafer.

16 September 2024 05:21:45

III. RESULTS AND DISCUSSION

An average of 20 data samples obtained from growths done over a range of PH_3 partial pressure (5 to 50 torr) were used to build the statistics for each growth temperature of 450

^{0}C, 540 ^{0}C, 650 ^{0}C, and 750 ^{0}C. Probability density distributions of peak position for different growth temperatures are plotted in Figure 3 (a) and fitted with skewed Gaussian functions. The quartile distribution of the peak position variation with growth temperature is shown in Figure 3 (b). It is observed that a growth temperature of 650 ^{0}C gives the narrowest dispersion around the median peak position very close to that of the single crystal wafer. Similar statistical analysis for FWHM and Urbach parameter were also performed and are

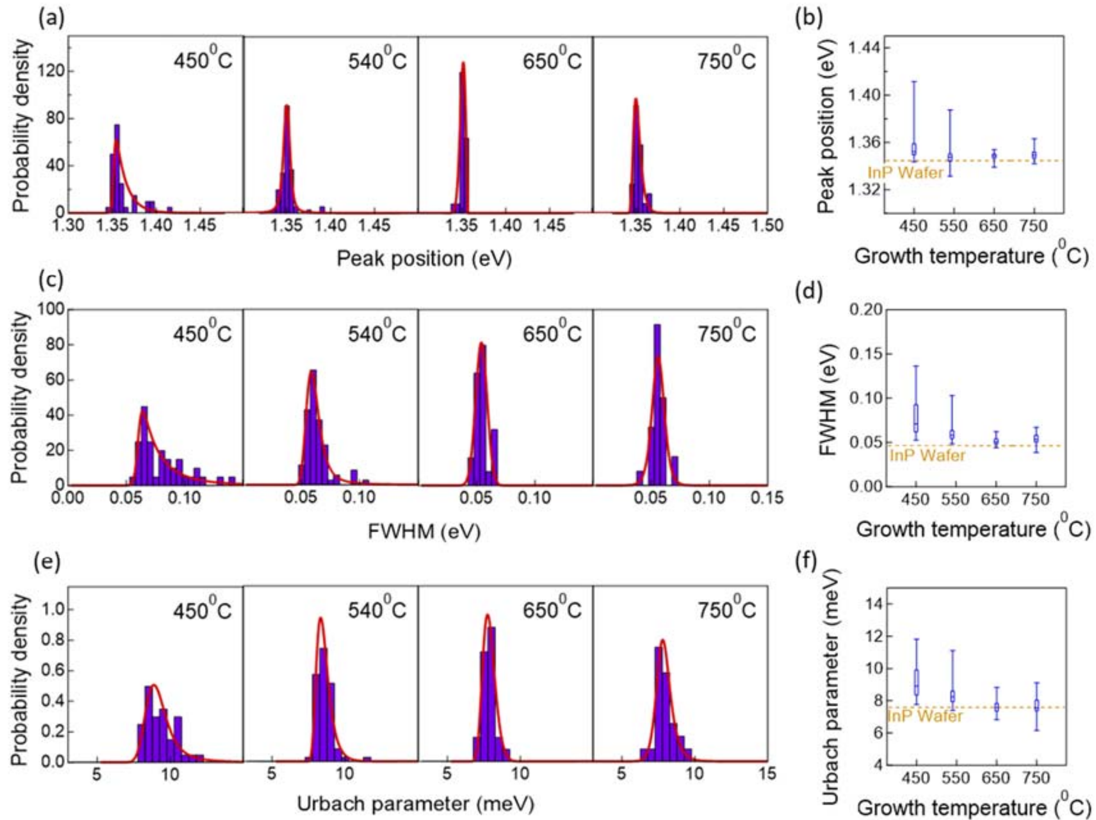

Figure 3. (Color online) Optoelectronic quality control through growth process optimization. Probability density distributions of (a) peak position, (c) FWHM, (e) Urbach parameter of InP templates grown on crystalline Gd_2O_3 film on Si at 450 ^{0}C, 540 ^{0}C, 650 ^{0}C, and 750 ^{0}C. Box-and-whisker quartile plots of (b) peak position, (d) FWHM, (f) Urbach parameter of InP grown on crystalline Gd_2O_3 film on Si at 450 ^{0}C, 540 ^{0}C, 650 ^{0}C, and 750 ^{0}C. Data of about 20 measurements are analyzed at each temperature.

16 September 2024 05:21:45

shown in Figures 3 (c) through (f).

For a clear visual comparison, the respective parametric values for the reference InP are also plotted in the corresponding quartile plots. Based on the holistic statistical analysis of the optoelectronic parameters, 650 ^{0}C appears to be an overall optimal growth temperature for vapor-liquid-solid InP templated films grown on Gd_2O_3.

Similar statistical analyses were also carried out on InP grown on other substrates, specifically graphene transferred on silicon dioxide (SiO_2) as shown in Figure 4 (a-c),

16 September 2024 05:21:45

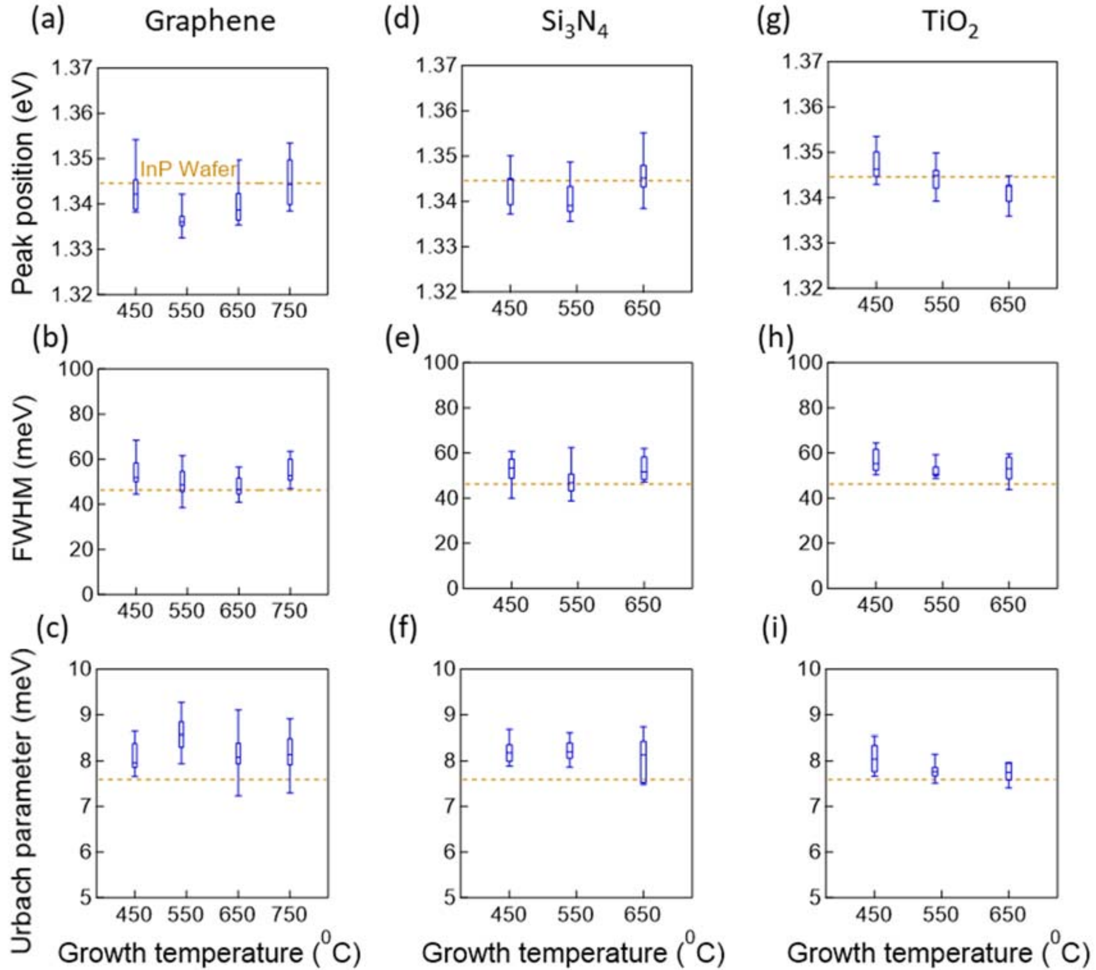

Figure 4. (Color online) Quartile plots for peak position, FWHM, and Urbach parameter for InP templates grown on (a-c) graphene, (d-f) Si_3N_4, (g-i) TiO_2 on Si/SiO_2 handle wafer.

16 September 2024 05:21:45

silicon nitride (Si_3N_4) shown in Figure 4 (d-f), and titanium dioxide (TiO_2) as shown in Figure 4 (g-i). In general, very narrow dispersion of the optoelectronic metrics namely peak position, FWHM, and Urbach parameter was observed for each substrate. It is important to observe that TLP InP of optoelectronic quality comparable to a single crystal InP wafer can be obtained in a growth temperature window of about 100^0C between 540^0C and 650^0C, independent of the chemical composition and microstructure of the substrate being used.

IV. SUMMARY AND CONCLUSIONS

In summary, we present a detailed optoelectronic characterization of InP grown on Si with TLP growth. Uniquely, we find that there is little variation of material quality across different buffer layers, paving the way for integration of crystalline materials without regard to substrate composition and crystal structure. This is in distinct contrast to current state of the art growth techniques, which are highly sensitive to the substrate and require complex growth techniques for integration with non-epitaxial substrates. Furthermore, we show that despite a simple growth reactor design, the overall variation of material quality within a growth run was narrow, indicating the scalability of this approach. Finally, through careful analysis of photoluminescence spectra of the TLP InP and a commercial single crystal InP wafer, we show the overall optoelectronic quality is similar. Future work may involve optoelectronic devices such as photodetectors, LEDs and lasers, and eventually photonic integrated circuits monolithically fabricated on dielectrics such as Si_3N_4 on Si.

16 September 2024 05:21:45

ACKNOWLEDGMENTS

R.K. acknowledges funding from the National Science Foundation (Award #1610604), NASA/JPL funding (Award #1571721), and Semiconductor Research Corporation (Award # 2018-NM-2799). D.S. thanks the support by the USC Annenberg Graduate Fellowship. J.T. thanks the support by the USC Provost Graduate Fellowship. J.R. acknowledges USC Viterbi School of Engineering Startup Funds and support from the Air Force Office of Scientific Research under award number FA9550-16-1-0335. The authors acknowledge the use of the Renishaw PL system in Dr. Stephen Cronin's lab and the electron imaging facilities at Center for Electron Microscopy and Microanalysis at USC.

REFERENCES

[1]G. B. Stringfellow, Organometallic vapor-phase epitaxy: theory and practice (Academic Press, 1999).

[2]A. Y. Cho and J. R. Arthur, Prog. Solid State Ch. **10,** 157 (1975).

[3]R. Kapadia, Z. Yu, H.-H. H. Wang, M. Zheng, C. Battaglia, M. Hettick, D. Kiriya, K. Takei, P. Lobaccaro, and J. W. Beeman, Sci. Rep. **3,** 2275 (2013).

[4]R. Kapadia, Z. Yu, M. Hettick, J. Xu, M. S. Zheng, C.-Y. Chen, A. D. Balan, D. C. Chrzan, and A. Javey, Chem. Mater. **26,** 1340 (2014).

[5]K. Chen, R. Kapadia, A. Harker, S. Desai, J. S. Kang, S. Chuang, M. Tosun, C. M. Sutter-Fella, M. Tsang, and Y. Zeng, Nat. Comm. **7,** 10502 (2016).

[6]Q. Lin, D. Sarkar, Y. Lin, M. Yeung, L. Blankemeier, J. Hazra, W. Wang, S. Niu, J. Ravichandran, Z. Fan, and R. Kapadia, ACS Nano **11,** 5113 (2017).

[7]D. Sarkar, J. Tao, W. Wang, Q. Lin, M. Yeung, C. Ren, and R. Kapadia, ACS Nano **12,** 1656 (2018).

[8]M. R. Shcherbakov, S. Liu, V. V. Zubyuk, A. Vaskin, P. P. Vabishchevich, G. Keeler, T. Pertsch, T. V. Dolgova, I. Staude, and I. Brener, Nat. Comm. **8,** 17 (2017).

[9]R. Nagarajan, C. H. Joyner, R. P. Schneider, J. S. Bostak, T. Butrie, A. G. Dentai, V. G. Dominic, P. W. Evans, M. Kato, and M. Kauffman, IEEE J. Sel. Top. Quant. **11,** 50 (2005).

[10]K. Hikosaka, U.S. Patent No. 5144378A (01 September 1992).

16 September 2024 05:21:45

[11]B. R. Bennett, R. A. Soref, and J. A. Del Alamo, IEEE J. Quantum Elect. **26,** 113 (1990).

[12]C. Liu, L. Dai, L. P. You, W. J. Xu, and G. G. Qin, Nanotechnology **19,** 465203 (2008).

[13]A. Iribarren, R. Castro-Rodríguez, V. Sosa, and J. L. Pena, Phys. Rev. B **58,** 1907 (1998).

[14]A. Iribarren, R. Castro-Rodriguez, V. Sosa, and J. L. Pena, Phys. Rev. B **60,** 4758 (1999).

[15]W. Van Roosbroeck and W. Shockley, Phys. Rev. **94,** 1558 (1954).

[16]A. Kost, H. C. Lee, Y. Zou, P. D. Dapkus, and E. Garmire, Appl. Phys. Lett. **54,** 1356 (1989).

[17]F. Urbach, Phys. Rev. **92,** 1324 (1953).

16 September 2024 05:21:45

FIGURE CAPTIONS

Figure 1. (Color online) (a-d) Schematic of TLP crystal growth process. (e-h) Optical microscope image of a representative template showing different stages of TLP crystal growth.

Figure 2. (Color online) (a) Cross-section TEM of InP on crystalline Gd_2O_3 film on Si. (b) Cross-section TEM of InP on amorphous TiO2 film on Si/ SiO_2. (c) Top-view SEM of InP templates on dielectric substrate. (d) Representative photoluminescence spectrum of USC InP compared with InP wafer.

Figure 3. (Color online) Optoelectronic quality control through growth process optimization. Probability density distributions of (a) peak position, (c) FWHM, (e)

Urbach parameter of InP templates grown on crystalline Gd_2O_3 film on Si at 450 ^{0}C, 540 ^{0}C, 650 ^{0}C, and 750 ^{0}C. Box-and-whisker quartile plots of (b) peak position, (d) FWHM, (f) Urbach parameter of InP grown on crystalline Gd_2O_3 film on Si at 450 ^{0}C, 540 ^{0}C, 650 ^{0}C, and 750 ^{0}C. Data of about 20 measurements are analyzed at each temperature.

Figure 4. (Color online) Quartile plots for peak position, FWHM, and Urbach parameter for InP templates grown on (a-c) graphene, (d-f) Si_3N_4, (g-i) TiO_2 on Si/SiO_2 handle wafer.

16 September 2024 05:21:45